Supporting information - Polarizability-dependent sorting of microparticles using continuous-flow dielectrophoretic chromatography with a frequency modulation method

Jasper Giesler [1], Georg R. Pesch [1,*], Laura Weirauch [1], Marc-Peter Schmidt [2], Jorg Thöming [1] and Michael Baune[1]

[1]   University of Bremen, Chemical Process Engeneering, Leobener Straße 6, 28359 Bremen, Germany
[2]   Brandenburg University of Applied Sciences, Department of Engineering, Magdeburger Straße 50, 14770 Brandenburg an der Havel, Germany
*   Correspondence: gpesch@uni-bremen.de

1   **Keywords:** Dielectrophoresis, DEP, microparticles, polystyrene, chromatography, interdigitated
2   electrodes, microfluidic, separation)

---

3   **1. Method**

4   Figure 1 shows the Re(CM) and mobility with respect to the frequency. Since the surface
5   conductance (here: $K_s = 1\,\mathrm{nS}$) is not easily measurable, these curves are assumptions and are used as
6   starting point for process parameters. For constant surface conductance and medium conductivity
7   the Re(CM) only depends on particle size. The chosen frequency band should include the cross-over
8   frequency of all particles to generate nDEP and pDEP.

9   **2. Device Fabrication**

10   *2.1. PDMS device*

11   The fabrication of PDMS microfluidic devices (soft lithography) is a well know process, which
12   was described in literature before [1,2]. A SU8-3050 master mold was produced using a laser printed
13   mask (25.000 dpi KOENEN GmbH, Germany, Figure 2 b) and standard photolithography techniques.
14   Afterwards, the PDMS channel can be made by pouring well mixed and degassed PDMS (10:1,
15   base:curing agent, Sylgard 184 Dow corning) onto the master mold. After curing the PDMS at 80 °C
16   for 1 h in a convection oven, the polymer can be cut into pieces as desired using a scalpel. Inlet and
17   outlet, both having an inner diameter of 1.5 mm, were punched using biopsy punches (Rapid-Core,
18   World Precision Instruments, Inc.).

19   *2.2. Electrodes*

20   The electrodes were fabricated using physical vapor deposition of first chrome as adhesion layer
21   and second gold as final layer. As substrate 100 mm borosilicate glass wafer were used. Afterwards,
22   using a chrome mask (100.000 dpi bvm.maskshop, Germany), positive photoresist and followed by a
23   wet etching process, the final electrodes were obtained. These electrodes had a witdh of 100 µm and
24   an identical gap width. To connect the amplifier to the flow cell contact pins were soldered onto the
25   electrode. The full electrode chip has length of 58 mm and a width of 26 mm (Figure 2 a).
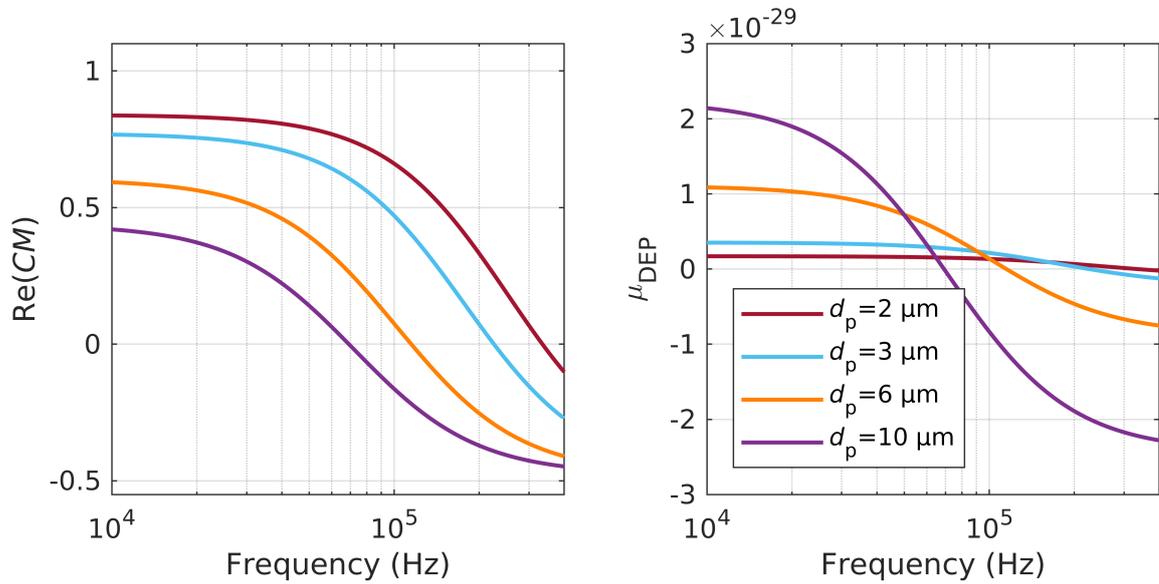
Figure 1. Real part of Clausius-Mossotti factor and dielectrophoretic mobility over frequency of the electric field of polystyrene particles ($d_\mathrm{p} = 2\,\mu\mathrm{m}$, $3\,\mu\mathrm{m}$ and $6\,\mu\mathrm{m}$). Particles suspended in DI water as surrounding medium, with $\sigma_\mathrm{m} = 1.2\,\mu\mathrm{S\,cm}^{-1}$ and $\varepsilon_\mathrm{m} = 78.5$).

a)   b)

Figure 2. a) Photography of the used gold electrodes with $100\,\mu\mathrm{m}$ electrode width & gap width b) Photomask for producing the SU8 master mold.

3. Post-processing

A segmentation algorithm was used to extract the fluorescence intensity of each colour of fluorescence into different images[3]. Afterwards the intensity of each image was calculated and a moving average was applied to reduce the level of noise of the measured intensities. Finally, the background signal was subtracted for each colour to eliminate scattered light and permanently adhered particles from the data. Since all measurements produce slightly different maximum values and each particle class has a different fluorescence intensity per particle, the Data was normalized by the maximum intensity value of each experiment.
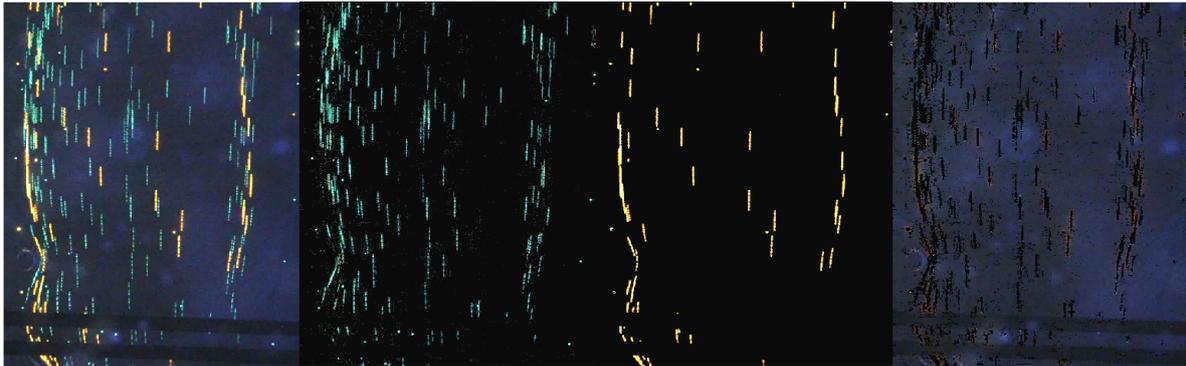
Figure 3. Result of the segmentation process. Original Image, particle typ 1, particle type 2 and background (f.l.t.r.)

4. Further experimental results

4.1. Full set of intensity profiles

4.1.1. Separation of 6 and 3 µm particles
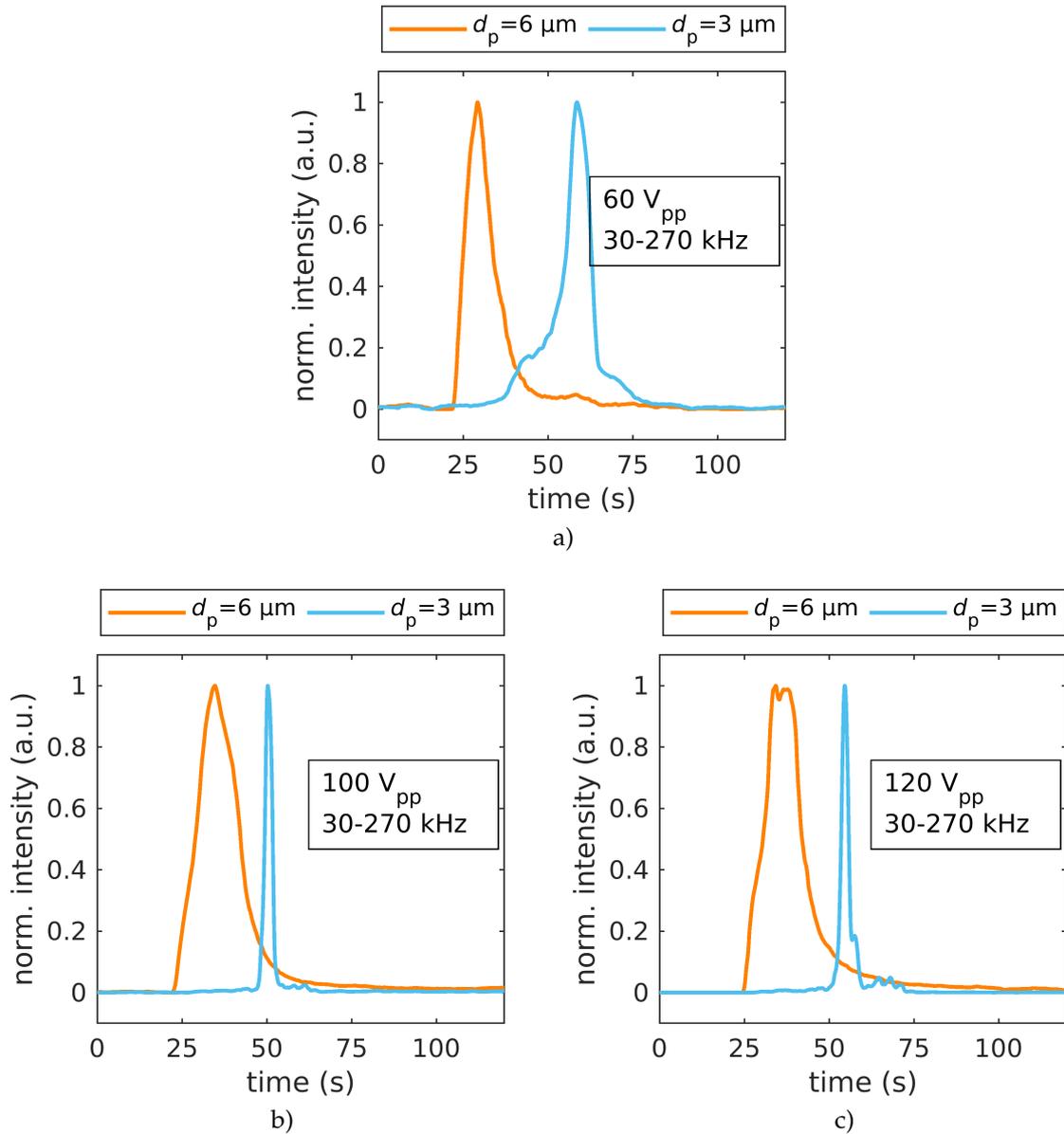
Figure 4. Fluorescence intensity over time of 3 µm and 6 µm fluorescent polystyrene particles at a) 60 V_{pp} b) 100 V_{pp} c)120 V_{pp} all experiments at 30 kHz - 270 kHz with a modulation frequency of 300 mHz

The separation of 3 µm and 6 µm fluorescent polystyrene particles at all voltages not shown in the main manuscript is show in Figure 4. For all applied voltages almost no retardation of the 6 µm particles could be observed, whereas for 3 µm the residence time diverges significantly from experiments without applied voltage. According to our calculations this separation is due to the retardation of the 3 µm particles, whose behaviour is dominated by pDEP.

42 4.1.2. Separation of 6 and 10 μm particles
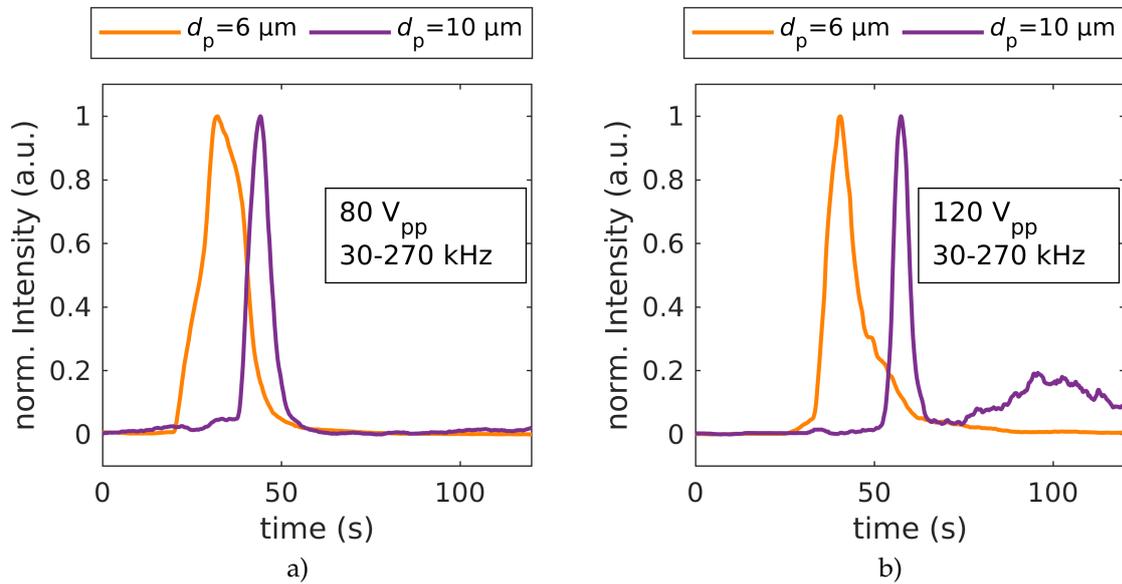
Figure 5. Fluorescence intensity over time of 6 μm and 10 μm fluorescent polystyrene particles at a) 80 V_{PP} and b) 120 V_{PP} all experiments at 30 kHz - 270 kHz with a modulation frequency of 300 mHz

43 To investigate the retention time of particles, which show, according to literature, substantial more
44 nDEP than pDEP, the separation of 6 μm and 10 μm was chosen. As addition to the data presented in
45 the main document the separation at 80 V_{PP} and 120 V_{PP} is presented in Figure 5.

46 4.1.3. Separation of 2 and 3 μm particles

47 The increase in resolution while increasing the applied voltage of the separation of 2 μm and 3 μm
48 fluorescent polystyrene particles is illustrated in Figure 8. With increasing voltage, the width decreases
49 and the peak maxima diverge progressively.
50 The variation of the set of frequencies (30 kHz - 270 kHz vs. 80 kHz - 320 kHz) is illustrated in
51 Figure 7 for 160 V_{PP}. The decrease in smaller retention time using 80 kHz - 320 kHz is shown in Figure 6.
52 The particles elute significantly later, when 30 kHz - 270 kHz are applied. The higher reetention time,
53 when using 30 kHz to 270 kHz, is due to less negative dielectrophoretic movement. Therefore, the
54 particles are more likley to stay in areas near to the electrode in which only low fluid velocity is present.
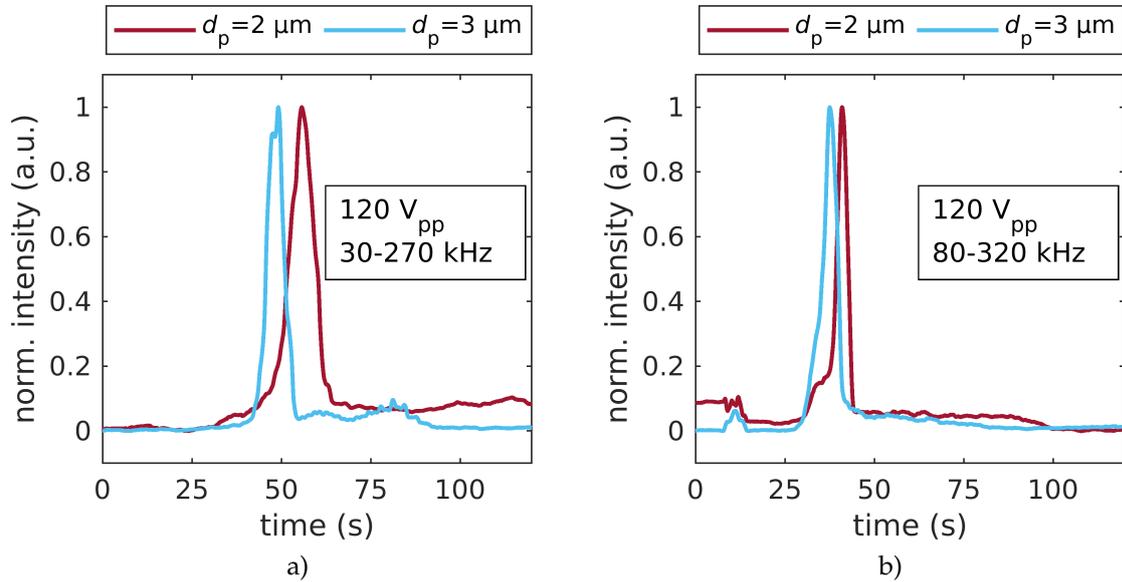
Figure 6. Fluorescence intensity over time of 2 µm and 3 µm fluorescent polystyrene particles. a) 120 V_{PP} at 30 kHz - 270 kHz b) 120 V_{PP} at 80 kHz - 320 kHz with a modulation frequency of 300 mHz
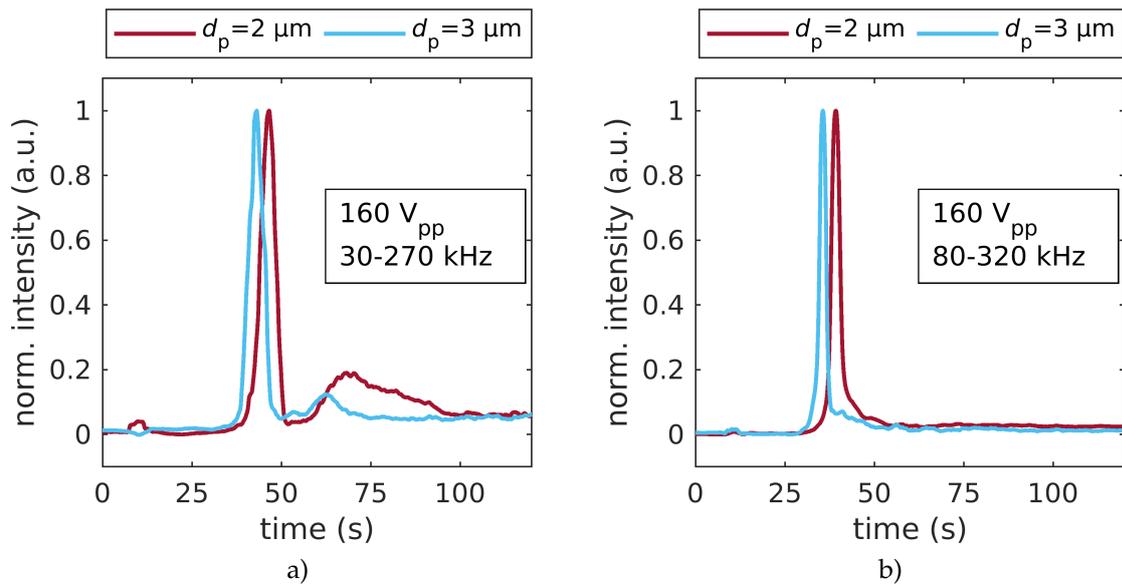
Figure 7. Fluorescence intensity over time of 2 µm and 3 µm fluorescent polystyrene particles. a) 160 V_{PP} at 30 kHz - 270 kHz b) 160 V_{PP} at 80 kHz - 320 kHz with a modulation frequency of 300 mHz
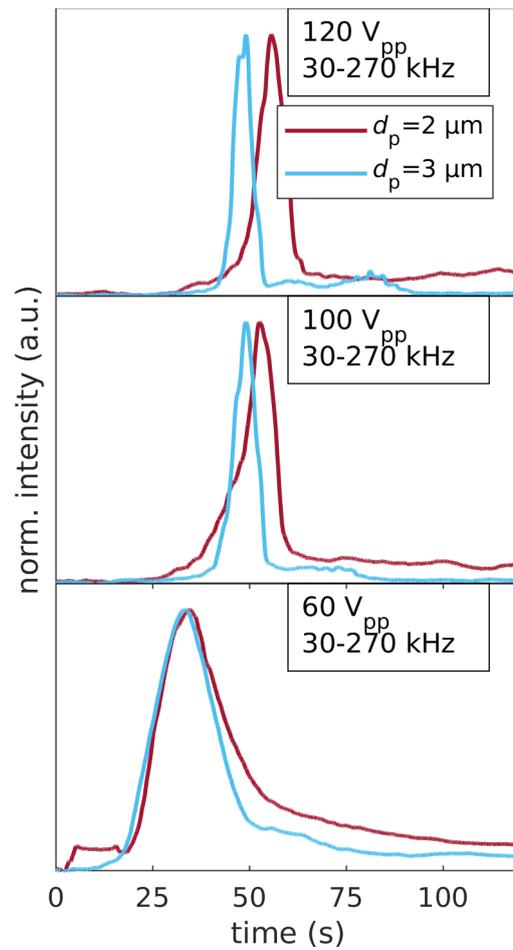
Figure 8. Fluorescence intensity over time of 2 µm and 3 µm fluorescent polystyrene particles with using different voltages. With increasing voltage the separation resolution R_s increases from $R_s(60\,V_{pp}) = 0.051 \pm 0.14$ to $R_s(100\,V_{pp}) = 0.24 \pm 0.07$ and finally to $R_s(120\,V_{pp}) = 0.54 \pm 0.1$ ($N = 4$ experiments)

4.2. Videos of separation and PIV data

4.2.1. PIV of 10 µm particles
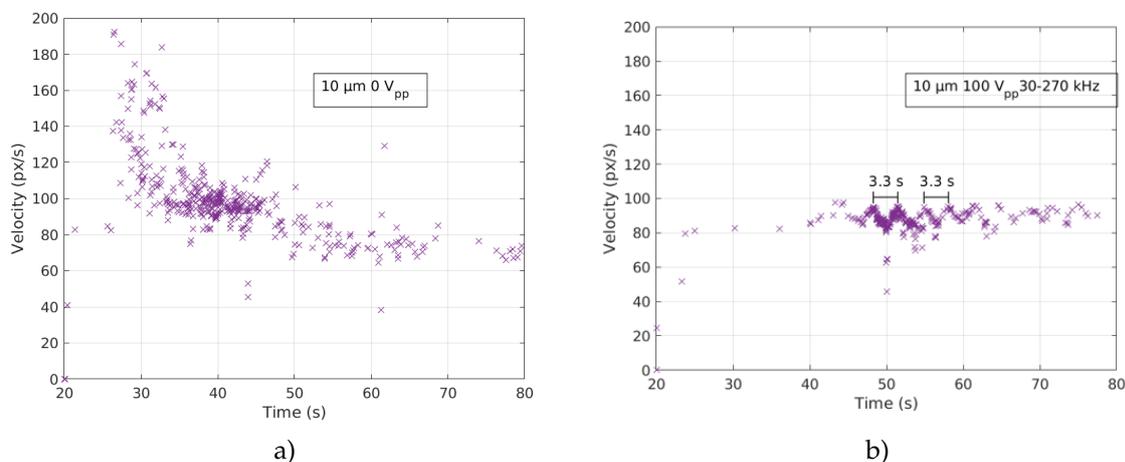
Figure 9. PIV Data of 10 µm PS particles at a) $0\,V_{pp}$ and b) $100\,V_{pp}$ at 30 to 270 kHz with a modulation frequency of 300 mHz. The measurement was performed at the outlet of the DPC channel, where no electrodes are present.

We conducted experiments with 10 µm at $0\,V_{pp}$ and $100\,V_{pp}$ to perform PIV measurements utilizing ImageJ and the TrackMate algorithm (s. Figure 9).

Without applying an electric field, at first fast particles arrive, whereas with increasing time slower particle elute from the channel. This is due to the laminar flow profile of the microchannel. When a voltage is applied, the velocity becomes more homogeneous and slower. The particles elute later from the channel and their velocity fluctuates with a 3.3 s period, which again is the cycle length of the frequency modulation. The fluctuation has an peak to peak value of about 15 px/s (80 to 95 px/s). The measurements were conducted at the outlet of the channel close to the last electrode the particles pass in the channel. No such periodic velocity change was observable for the 6 µm particles (which were still big enough to perform PIV measurements). We have also added a video "10um_100Vpp_PIVdata.mp4" to the Supplement from which the PIV data was evaluated. However, the periodic velocity changes are too small to observe them with the bare eye.

4.2.2. Videos for 3 µm and 6 µm particles

For smaller particles no PIV measurements were possible, due to their low fluorescence intensity. However, videos ($0\,V_{pp}$: "DPC_0Vpp_3vs6umPS.mp4" & $80\,V_{pp}$: "DPC_80Vpp_3vs6umPS.mp4") are available as Supporting Documents of the separation of 3 and 6 µm particles with subtitles in it to guide the eye. The videos are cropped and adjusted in contrast, colour and brightness for better visibility. For future work a more powerful light source/laser could be used to generate a more detailed set of PIV data. These videos clearly show how the 3 µm particles slow down in intervals that match the applied frequency modulation. The videos were taken at the outlet of the channel close to the last electrode the particles pass in the channel.

1. Tu, J.; Qiao, Y.; Feng, H.; Li, J.; Fu, J.; Liang, F.; Lu, Z. PDMS-based microfluidic devices using commoditized PCBs as masters with no specialized equipment required. *RSC Adv.* **2017**, *7*, 31603–31609. doi:10.1039/c7ra03899b.
2. Faustino, V.; Catarino, S.O.; Lima, R.; Minas, G. Biomedical microfluidic devices by using low-cost fabrication techniques: A review. *J. Biomech.* **2016**, *49*, 2280–2292, [_barata Materials and Techniques of polychrome wooden sculpture]. doi:10.1016/j.jbiomech.2015.11.031.
3. MathWorks. Color Based Segmentation Using the L * a * b * Color Space, 2019.